BMC Medicine

RESEARCH

Open Access

Sexual dimorphism in the association of umbilical cord blood lipidome with abdominal fat in early childhood

Kothandaraman Narasimhan[1*], Mya Thway Tint[1], Li Chen[1,2], Sartaj Ahmad Mir[2,3], Suresh Anand Sadananthan[1], Navin Michael[1], Adaikalavan Ramasamy[4], Karen Mei-Ling Tan[1], Priti Mishra[1], Anne K. Bendt[2], Kok Hian Tan[5], David Cameron-Smith[1,6], Yap Seng Chong[1,7], Peter D. Gluckman[1,8], Peter J. Meikle[9,10], Melvin Khee Shing Leow[1,6,11,12,13], Fabian Yap[14], Yung Seng Lee[15], Chan Shiao Yng[1], Johan G. Eriksson[1,7,16,17], S Sendhil Velan[1], Neerja Karnani[1,3,18] and Markus R. Wenk[2,3,19*]

Abstract

Background Although the associations between cord blood lipidome and neonatal birth weight are established, it remains uncertain whether sexual dimorphism in fetal fat accumulation extends to the relationship between cord blood lipid profiles and neonatal abdominal fat compartments. Understanding these relationships could provide insights into early sex-specific differences in lipid metabolism.

Methods We conducted lipidomics of umbilical cord blood plasma samples (350 (46.6%) girls and 401 (53.4%) boys) from the Growing Up in Singapore Towards healthy Outcomes (GUSTO) birth cohort. Abdominal fat compartments—superficial subcutaneous adipose tissue (sSAT), deep SAT (dSAT), and intra-abdominal adipose tissue (IAT)—were quantified by magnetic resonance imaging within 2 weeks of birth in 239 subjects. Linear regression models were used to assess sex differences in lipid species associated with abdominal fat compartments.

Results Newborn girls had significantly higher superficial and deep subcutaneous adipose tissue volumes compared to boys, whereas intra-abdominal adipose tissue volumes were similar between sexes. In the pooled analysis, cord blood plasma lipids showed distinct associations with different fat depots: 38 lipid species were associated with sSAT, 4 with dSAT, and 38 with IAT. In sex-stratified analyses, 13 lipids were associated with sSAT in girls and 3 in boys, whereas dSAT showed associations with 45 lipids in boys but none in girls. These sex differences were primarily observed in ether-linked phospholipids and ceramides. Notably, no significant associations were observed between lipids and IAT in either sex, suggesting depot-specific sexual dimorphism in early life.

Conclusions Our study reveals sexual dimorphism in the associations between cord blood lipidome and abdominal adiposity, suggesting depot-specific patterns in adipose tissue development and lipid metabolism in early life.

Keywords Umbilical cord blood, Lipidomics, Subcutaneous adipose tissue, Deep subcutaneous adipose tissue, Superficial subcutaneous adipose tissue, Visceral adipose tissue

*Correspondence:
Kothandaraman Narasimhan
Kothandaraman_Narasimhan@sics.a-star.edu.sg
Markus R. Wenk
bchmrw@nus.edu.sg
Full list of author information is available at the end of the article

Background

Sex differences in body composition are present from birth, with differences in fat mass (e.g., sSAT) documented in neonates [1]. These differences become more pronounced during early infancy, particularly during the mini-puberty period when male infants experience increased testosterone production [2]. As development continues, distinct patterns of fat distribution emerge, with females showing a greater tendency for gluteofemoral fat accumulation and males showing greater central/truncal fat distribution [3]. These patterns appear to be influenced by both early life factors and later developmental stages. Adaptations in lipid metabolism during the early stages of human development may influence weight and body composition status in infants [4, 5]. Understanding the role of sexual dimorphism in the development of neonatal body fat distribution in boys and girls could help in understanding the physiological differences associated with lipid metabolism in the two sexes. Circulating plasma lipidome is strongly associated with sex in adults [6–8]. In adults, the plasma lipidome exhibits notable sex-specific differences, with variations across different lipid classes and species, influenced by a complex interplay of genetic, hormonal, and lifestyle factors [9]. Males typically show higher levels of triglycerides, particularly in very-low-density lipoprotein (VLDL) particles, and also higher levels of lysophospholipids, whereas females tend to have higher levels of low-density lipoprotein (LDL) cholesterol, as well as higher levels of glycerophospholipids such as phosphatidylcholine (PC) and phosphatidylethanolamine (PE) [10]. Furthermore, certain sphingolipids, particularly those containing the d18:2 sphingoid base, are found in higher concentrations in women [11]. However, the role of cord blood plasma lipids on fetal fat accumulation remains largely unknown [12, 13]. Further, there is paucity of studies focusing on specific fat compartments (abdominal adipose tissue volumes) and their association with the cord blood circulating lipids. This study aims to characterize the sex-based differences in the associations of cord lipids with neonatal abdominal fat compartments in a prospective Asian birth cohort.

Methods

Study participants and clinical characteristics

GUSTO (Growing Up in Singapore Towards healthy Outcomes) is a prospective mother–offspring birth cohort study in Singapore which recruited 1450 women during early pregnancy between June 2009 and September 2010 at KKH and National University Hospital (NUH) maternity units [14]. Study participants were of Chinese, Malay, or Indian ethnicities with homogeneous parental ethnic backgrounds. Ethics approval for the study was granted by the Domain Specific Review Board of Singapore National Healthcare Group (reference D/09/021) and the Centralised Institutional Review Board of SingHealth cluster (reference 2009/280/D). Written informed consent was obtained at recruitment for mothers and their offsprings' participation in this study. Demographic and lifestyle factors of mothers such as maternal age, ethnicity, education level, and self-reported pre-pregnancy weights were collected by interviewer-administered questionnaires. The pre-pregnancy BMI (ppBMI) was calculated as the self-reported pre-pregnancy weight in kilograms divided by the square of the measured height in meters [15]. Total gestational weight gain was calculated by subtracting pre-pregnancy weights from weights measured at the end of pregnancy. Information related to neonates such as gestational age, birth weight, and sex were retrieved from hospital delivery records. Birth lengths were measured by trained research staff within 72 h of delivery.

Lipidomics analysis

Plasma lipidomics was conducted as described previously [16]. Lipid extraction was carried out using butanol: methanol (extraction solvent) in a ratio of 1:1 containing 10 mM ammonium formate and lipid class specific internal standards. A total of 100 µL of extraction solvent was added to each sample, vortexed for 10 s followed by sonication for 60 min with temperature maintained at 18–22 °C. The samples were centrifuged at a speed of 13,000 rpm for 10 min. The supernatant (80 µL) was collected in mass spectrometry-compatible vials and stored at − 80 °C for LC–MS/MS. These lipid extracts were analyzed by using Agilent 6490 QQQ mass spectrometer interfaced with an Agilent 1290 series UHPLC system. Lipids were separated on a ZORBAX RRHD UHPLC C18 column (2.1 × 100 mm 1.8 mm, Agilent Technologies) with the thermostat set at 45 °C. Targeted LC–MS/MS was performed in ESI positive ion mode with dynamic multiple reaction monitoring (dMRM). The MassHunter Quantitative software (Agilent Technologies) was used for data integration and the peak area of each analyte was exported as.csv files for further analysis in R software. Quality control samples (prepared by pooling study samples) were analyzed along with the study samples to monitor sample extraction efficiency as well as LC–MS/MS performance and were subsequently used to do batch corrections. Quantification was carried out by normalizing the peak area of lipids to the respective internal standards. Lipid species were dropped if the quality control coefficient of variation was greater than 20%. Finally, a total of 480 lipid species representing 25 lipid classes were used for further analysis.

Offspring birth weight and adiposity measurements at birth

Magnetic resonance imaging (MRI) was performed on neonates within two weeks after birth (mean age (SD): 9.5 (2.8) days) using a GE Signa HDxt 1.5 T MR scanner (GE Healthcare). Under neonatologist supervision, naturally sleeping neonates were positioned in an immobilization device on an adult head coil. Abdominal imaging was performed using a T1-weighted water-suppressed fast spin-echo sequence, covering the abdomen from the diaphragm to the symphysis pubis. Images were acquired during free breathing, which resulted in respiratory artifacts. To address this, the data were initially processed using an in-house semi-automated quantitative analysis algorithm with MATLAB 7.13 (The MathWorks Inc., Natick, Massachusetts, USA). The resulting output images were carefully reviewed and manually corrected for mis-segmentations by trained MR readers under radiologist guidance. The methodology for segmenting sSAT, dSAT, and IAT were reported earlier [17].

Statistical analysis

Analyses for lipid association with the abdominal adipose tissue volumes were carried out at the lipid species and class levels. Total lipid class concentration was calculated by summing up the concentration of individual lipid species within each class. The lipidomics data were $\log_{10}$ transformed for statistical analyses. For analyzing associations of cord blood plasma lipidome with sSAT, dSAT, and IAT, abdominal fat compartment volumes were regressed (linear regression models) against $\log_{10}$ transformed concentrations of each lipid and adjusted for ethnicity, maternal fasting plasma glucose (pregnancy week 26), mother's age at recruitment, education, parity, pre-pregnancy BMI, total GWG, gestational age at delivery, sex and age on the day of MRI in individual regression models. The regression coefficients (β) were expressed as a change in fat volume in mL per 10% increase in lipid concentration (change in fat volume (sSAT, dSAT, and IAT). We also examined whether sex could modify the association by incorporating lipid × sex interaction terms into the corresponding adjusted model. Sex-specific associations between cord blood lipidome and adipose tissue compartments were evaluated using two complementary approaches. First, lipid × sex interaction terms were incorporated into the adjusted regression models to test for sex-specific effect modification. Second, sex-stratified analyses were performed to obtain sex-specific effect estimates. This dual analytical strategy was implemented to both detect statistically significant sex differences in lipid-adipose tissue associations (interaction analysis) and quantify the magnitude and direction of associations within each sex group (stratified analysis). In the sex-stratified analyses, adjustments were made for the same covariates as the main models, with sex inherently accounted for through stratification. The adjusted p-values were calculated by the Benjamini-Hochberg (BH) method for multiple testing correction [18]. Statistical significance was assessed using a two-sided significance level of $\alpha = 0.05$. For the multiple comparison analyses, lipid associations were considered statistically significant if they met the threshold of adjusted p-value < 0.05 after BH correction. For the sex interaction analyses, interactions were considered significant at $p < 0.05$. Forest plots were employed to illustrate the effect sizes of individual lipid species, categorized by class, and their associations with the three abdominal body fat compartments and differences between male and female neonates. All statistical analyses were performed using R (version 4.1.1). Figures were generated using the ggplot 2 package in R [19].

Results

In the current study, a cohort of 751 newborns, comprising 401 boys and 350 girls with available cord blood lipidome data, was assessed for eligibility. Out of this cohort, 239 neonates (131 boys and 108 girls) had both comprehensive cord blood lipid data and underwent neonatal MRI scans, as detailed in Fig. 1. Birth weights ranged from 2.01 kg to 4.1 kg, with boys having a slightly higher mean birth weight of 3.15 (SD ± 0.44) kg compared with the girls' mean of 3.05 (SD ± 0.4) kg ($p = 0.08$) (Table 1).

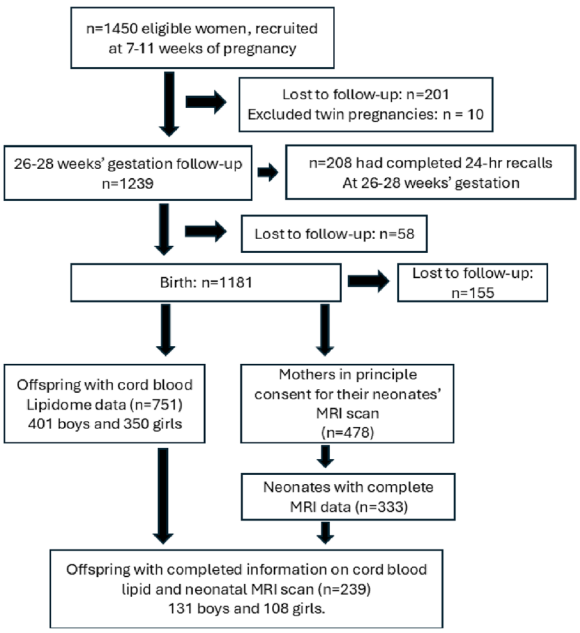

Fig. 1 Workflow of the current study

Table 1 Maternal and offspring characteristics in the GUSTO study

	Male $N=131$	Female $N=108$	*p*-value
Maternal characteristics			
Ethnicity, *N* (%)			0.6
Chinese	50 (38%)	47 (44%)	
Malay	55 (42%)	39 (36%)	
Indian	26 (20%)	22 (20%)	
Age in years at recruitment, mean (SD)	29.29 (5.24)	28.38 (5.44)	0.2
Highest level of education attained, *N* (%)			0.14
Primary and secondary	48 (37%)	53 (50%)	
Post-secondary	58 (45%)	39 (37%)	
University	23 (18%)	14 (13%)	
Fasting plasma glucose 26–28 weeks gestation (mmol/L), mean (SD)	4.42 (0.60)	4.42 (0.59)	> 0.9
2 h plasma glucose at 26–28 weeks gestation (mmol/L), mean (SD)	6.44 (1.64)	6.23 (1.48)	0.3
Pre-pregnancy BMI in kg/m^2, mean (SD)	23.10 (4.84)	23.47 (5.51)	0.6
Gestational age in weeks, mean (SD)	38.64 (1.28)	38.95 (1.15)	0.05
Parity			0.03
Multiparous	27 (21%)	25 (23%)	
Nulliparous	46 (35%)	53 (49%)	
Primiparous	58 (44%)	30 (28%)	
Gestational weight gain (kg), mean (SD)	13.89 (5.82)	14.30 (6.88)	0.7
Offspring characteristics			
Birth weight in kg, mean (SD)	3.15 (0.44)	3.05 (0.40)	0.08
Cord blood lipidome (N)	401	350	
Cord blood lipidome and neonatal MRI for adiposity (N)	131	108	
Age in days at neonatal MRI, mean (SD)	9.76 (2.65)	9.72 (3.09)	> 0.9

Maternal demographics and clinical characteristics were mostly similar to those of the samples excluded from the study (Additional file 1: Table S1).

The newborn abdominal adipose tissue fat compartments revealed sex-specific differences (Fig. 2). Boys exhibited lower volumes of sSAT averaging 74.05 ± 20.28 mL, as compared with girls who averaged 81.66 ± 21.83 mL ($p < 0.006$). Additionally, the dSAT volume in boys was also lower at 12.67 ± 5.50 mL whereas girls had a volume of 14.27 ± 5.76 mL ($p < 0.03$).

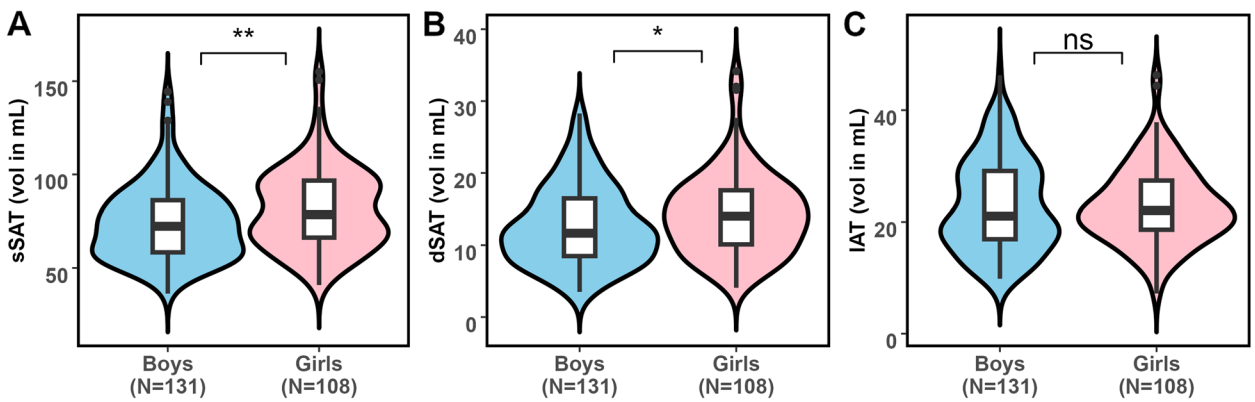

Fig. 2 Distribution of sSAT, dSAT, and IAT volumes (in mL) by offspring sex. Violin plots show the distribution of (**A**) sSAT, (**B**) dSAT, and (**C**) IAT volumes in boys (blue, $n = 131$) and girls (pink, $n = 108$). Sex-specific differences were observed in sSAT (**$p < 0.01$) and dSAT (*$p < 0.05$) volumes, while no significant differences were observed for IAT volumes (ns: not significant)

In contrast, IAT volume showed minimal difference between the sexes, with values being 22.98 ± 8.18 mL for boys and 22.92 ± 6.88 mL for girls ($p > 0.9$) (Fig. 2).

Correlations between fat depots and total body weight, and between different fat depots in boys and girls

Sex-stratified analysis revealed distinct correlation patterns between abdominal fat compartments (Additional file 1: Table S2). In males, strong correlations were observed between sSAT and dSAT ($R = 0.83$), while moderate correlations were found between sSAT and IAT ($R = 0.68$), and dSAT and IAT ($R = 0.66$). Female participants showed similar but slightly lower correlation coefficients, with sSAT and dSAT correlation at $R = 0.80$, sSAT and IAT at $R = 0.70$, and dSAT and IAT at $R = 0.62$. Total body weight showed moderate-to-strong correlations with all fat depots (Additional file 1: Table S3), with the strongest association observed with sSAT ($R = 0.75$), followed by dSAT ($R = 0.67$) and IAT ($R = 0.64$). This pattern suggests a hierarchical relationship between fat depot distribution and total body mass, with superficial subcutaneous adipose tissue showing consistently stronger associations with both total adiposity and body weight compared to other fat compartments.

The association between body fat depot volumes and cord blood lipidome in neonates

In the pooled analysis, 38 lipid species were associated with sSAT, 4 lipid species with dSAT, and 38 lipid species with IAT (Fig. 3A-C, Additional file 1: Table 6A). Lysophosphatidylcholine, LPC(16:1) (sn2) and LPC(16:1) (sn1), were common to all three fat depots (Additional file 2: Fig. S1 and Additional file 1: Table S4). Among the fat depots, dSAT had the fewest unique lipid species, which belonged to the TG class. The common lipids associated with sSAT and IAT consisted of lysophosphatidylcholine, lysophosphatidylethanolamine, and triglyceride lipid classes. At the total class level, triglycerides were negatively associated (with dSAT and IAT) and lysophospholipids were positively associated with body fat depots (Fig. 3E–F; Additional file 1: Table S6B). The fat depot sSAT was unique in its positive association with lysophospholipids, whereas dSAT was associated with both lysophospholipids and triglycerides. Similarly, IAT was also mainly associated with lysophospholipids and triglycerides. In this study, 16 babies were born between gestational weeks 35 and 37. Excluding them did not affect the results (Additional file 2: Fig. S3).

Sex differences in the associations between abdominal fat volumes and cord blood lipids

Next, in models combining both sexes to examine associations of cord blood plasma lipidomic signatures and abdominal adipose tissue volumes, sex-specific interaction was observed. For sSAT, 27 individual lipid species showed a sex-interaction (interaction $p < 0.05$) (Fig. 4A and B; Additional file 1: Table S5 and Additional file 1: Table S6C); Phospholipids containing long chain PUFAs, specifically FA20:5, FA22:5, and FA22:6 showed sex-specific interactions. For sSAT LPC(22:5) (n3) and LPC(22:5) (n6) were significant after multiple corrections (Fig. 5). In contrast, fewer lipids showed sex-specific interactions with dSAT and IAT fat depots. For dSAT, only 15 lipids showed sex-interaction (interaction $p < 0.05$), mostly triglycerides containing FA18:3 and LPC 22:5. In terms of directionality, these lipid associations followed a similar pattern to what was observed for sSAT, reaffirming the interaction was consistent across the three fat depots. Nonetheless, the three depots did not share any common lipids for sex-interaction (Additional file 2: Fig. S2 and Additional file 1: Table S5), but a subset of lipids exhibiting sex-specific associations was found to be common between sSAT and dSAT, with the majority being lysophospholipids and ether-linked phospholipids.

Sex-stratified association analysis between cord blood plasma lipidome and volume of abdominal fat compartments

The sex-stratified analysis showed differences in the cord blood plasma lipids that were associated with the volume of abdominal fat depots in boys and girls. These sex-specific differences in associations were observed for all the three fat depots. Three lipids were associated with sSAT volume in boys, whereas thirteen lipids were associated with sSAT volume in girls (Additional file 2: Fig. S4; Additional file 1: Table S6E). Among the associated lipids, LPC(16:1) (sn1) and LPC(16:1) (sn2) were common to both boys and girls. Lysophospholipid classes including LPE, LPC, and LPC(O) were positively associated and deoxyceramide and triglycerides were negatively associated with sSAT volume in boys whereas only LPE and LPC classes were positively associated in girls (Additional file 2: Fig. S4B; Additional file 1: Table S6E). For dSAT volume, a higher number of lipids showed association in boys (Additional file 2: Fig. S5A; Additional file 1: Table S6E); forty-five lipids, mostly triglycerides exhibited an inverse association in boys (37/45; 82.2%). No significant association between lipids and dSAT volume was observed in girls (at FDR < 0.05). For IAT, we found no significant associations (FDR < 0.05) in either boys or girls, suggesting distinct metabolic characteristics of this depot compared to subcutaneous fat compartments (Additional file 2: Fig. S6; Additional file 1: Table S6E). At the total lipid class level, except for sSAT girls, no other significant associations were observed (Additional file 2: Fig. S4D; Additional file 1: Table S6F).

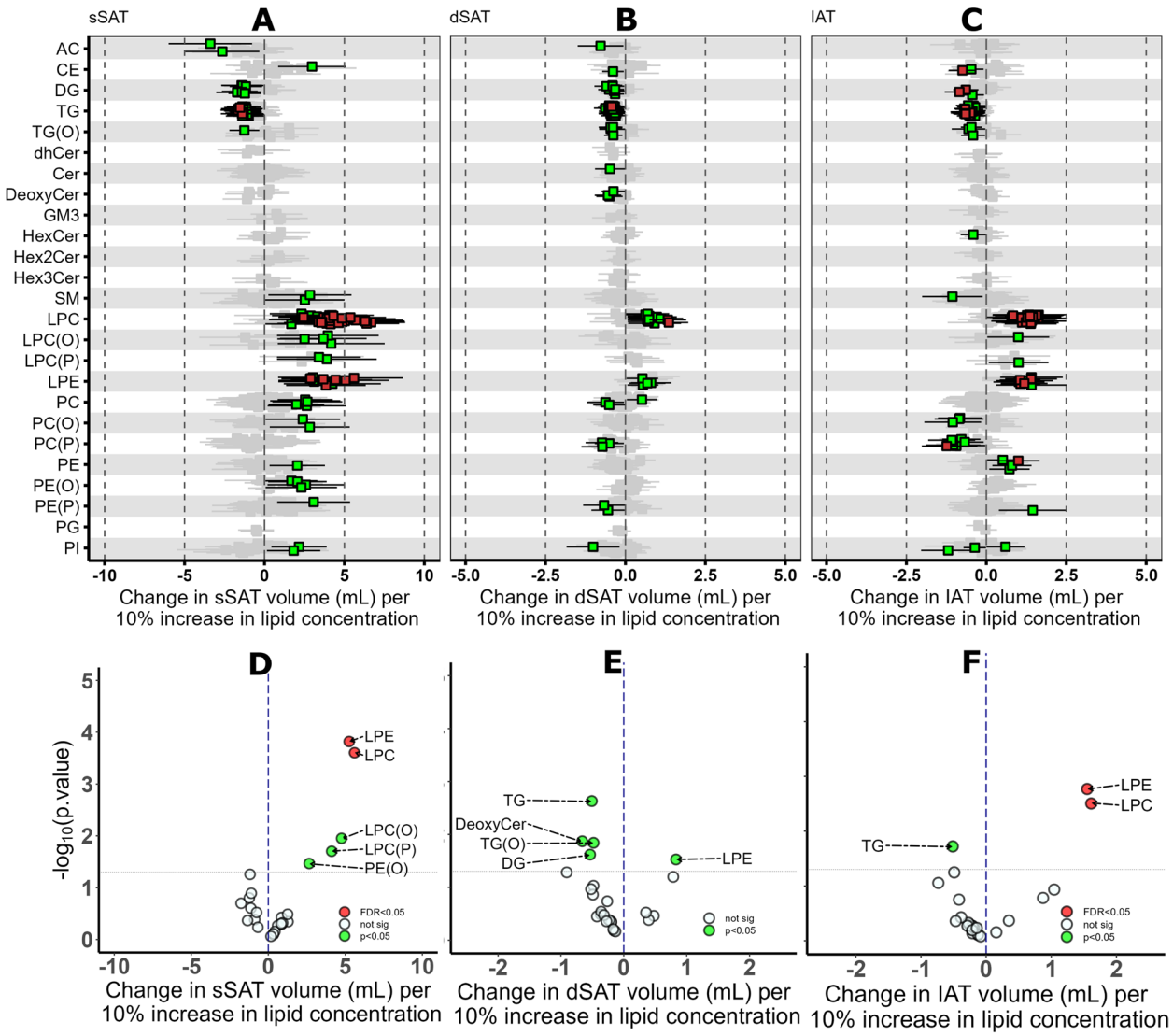

Fig. 3 Forest plot showing linear regression analysis between body fat depots sSAT, dSAT, and IAT and log-transformed lipid concentration (**A**–**C**) and volcano plot for lipid classes (**D**–**F**). Gray circles show nonsignificant lipid species, and green and red closed circles show species with $p < 0.05$ and species with FDR < 0.05, respectively. Error bars represent the 95% confidence interval

We examined the associations between cord blood lipids and total abdominal adiposity, and whether these associations with the fat depots were independent of birth weight. The relationships between cord blood lipids and TAAT showed patterns similar to those observed in individual fat depots: LPC and LPE showed strong positive associations, whereas TGs showed negative associations and other phospholipids demonstrated modest associations (Additional file 2: Fig. S7A–F). The direction and significance of these associations remained consistent across both individual depots and total adiposity. After including birthweight into the model, most associations were attenuated across all fat depots (Additional file 1: Tables S6G–J). Specifically, in sSAT, only two lipid species maintained significant associations in girls: LPC(22:5)sn1/LPC(22:5)sn2 and LPC(22:5)(n3) (sn1) (104_sn1), while no significant associations persisted in boys. For both dSAT and IAT, no significant associations remained after birthweight adjustment in either girls or boys. Notably, adjusting for birthweight may not be appropriate in this analysis since fat mass (including abdominal fat compartments) and fat-free mass are primary components of birthweight itself. This represents a potential case of overadjustment bias [20], where including birthweight as a covariate could systematically bias the effect estimates toward the null, thereby obscuring

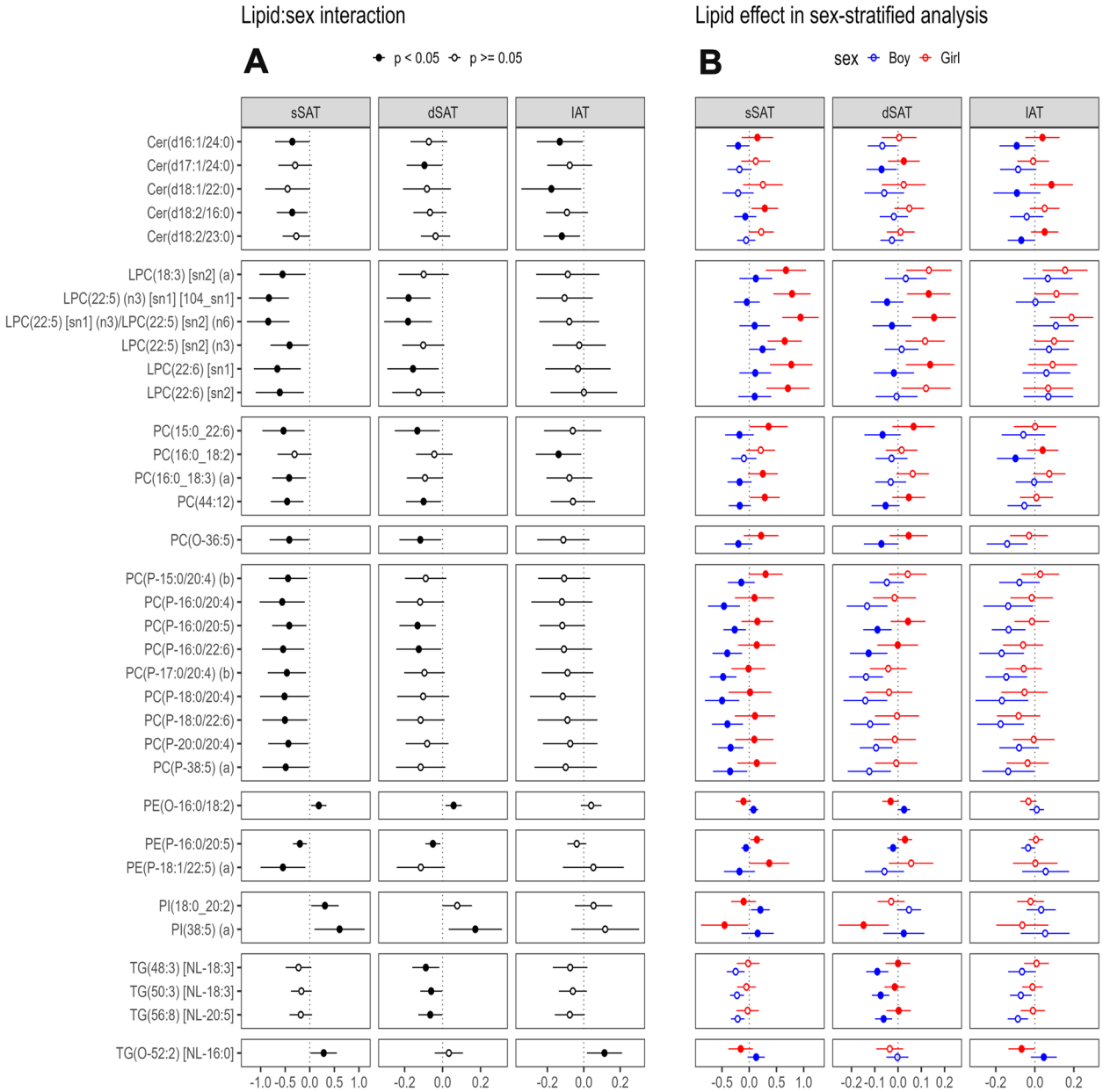

Fig. 4 Sex-interaction of cord blood lipids and fat depots. Sex-interaction of cord blood lipids and fat depots. **A** Beta (β) for the interaction between lipid levels and sex. A positive value of β suggests the lipid association is relatively stronger in boys compared to girls and vice versa. Filled circles denote interaction terms with p-values < 0.05. **B** β for the lipid association in boys (blue) and girls (red). Filled circles indicate pairs where the difference (i.e., lipid × sex interaction term) has a $p < 0.05$

true biological associations between cord lipids and fat depots.

Discussion

Our comprehensive analysis revealed distinct lipidomic signatures of sSAT, dSAT, and IAT suggesting metabolic compartmentalization of abdominal fat depots at birth. Cord blood lipids reflect a complex interplay of maternal–fetal lipid transfer [16, 21–24], fetal lipid metabolism and storage [5], and potential lipid mobilization during the birth process [4, 25]. These factors highlight the dynamic exchange between the mother and fetus, and the fetus responses to the intrauterine environment [16]. Within this context, our analysis revealed that all three fat depots exhibited positive associations with LPCs, with LPC(16:1) showing consistent positive

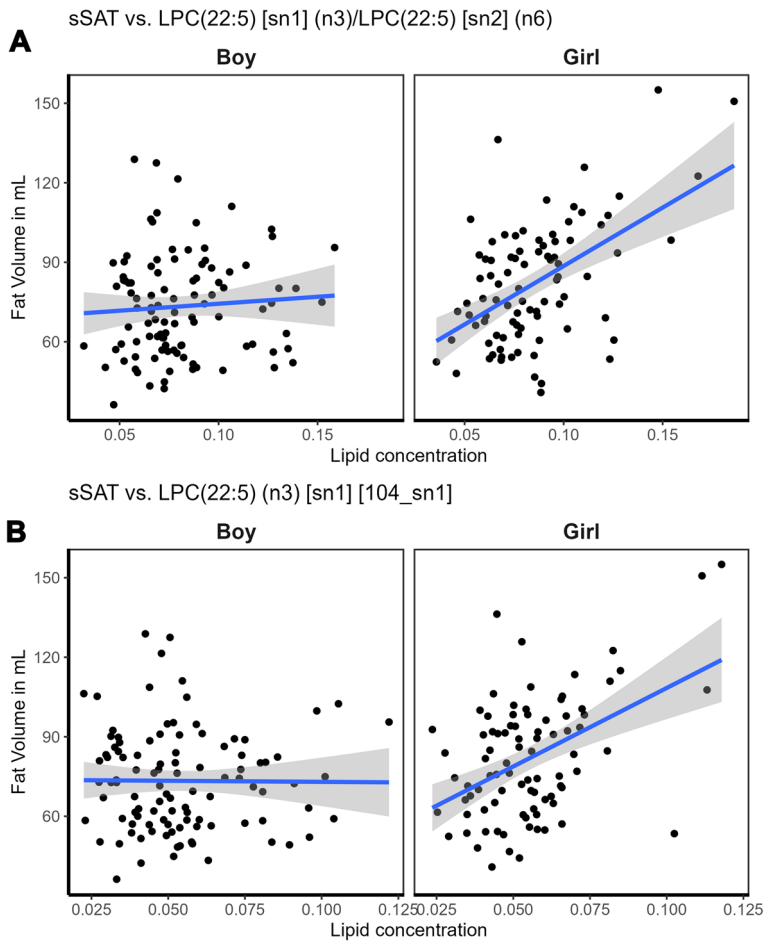

Fig. 5 Interaction plots of lipids that showed significance at FDR < 0.05 in the association of lipids and sSAT volume in boys and girls

associations across all depots. These findings align with previous studies demonstrating associations between cord blood LPC(16:1) and birthweight [5, 21, 26]. One possible mechanism that could explain the positive association between LPCs and birth weight involves enhanced lipogenesis potentially mediated by increased stearoyl-CoA desaturase-1 (SCD1) activity [21]. At birth, infants accumulate adipose tissue at high rates and can reach up to 25% of body weight by 4–5 months. Apart from being essential for membrane architecture and secretory functions, LPCs serve as biological signals regulating essential fetal growth and development [27]. The strong positive associations observed between LPC(16:1) and neonatal fat depot volumes highlight an essential role of palmitoleic acid in adipose tissue development. Taken together, these data suggest the role of increased endogenous lipogenesis in early childhood adipose tissue accumulation and compartmentalization. Beyond LPC(16:1), multiple LPC species, containing FA18:1, FA22:4, and FA20:2, demonstrated robust positive associations with sSAT, suggesting their potential involvement in sSAT development. Furthermore, LPEs showed consistent positive associations with both IAT and sSAT compartments, specifically those with FA18:1, FA18:2, and FA20:4 species, indicating their potential regulatory role in depot-specific adipogenesis. The dSAT demonstrated a more restricted association profile compared to other depots, predominantly exhibiting associations with LPC(16:1) and a few triglyceride species, suggesting distinct metabolic regulation in this intermediate adipose layer. Levels of cord plasma diglycerides and triglycerides were generally negatively associated with the volumes of the three fat depots. In contrast to the association of plasma triglycerides with adiposity measures in adults, cord blood triglycerides have been shown to be negatively associated with neonatal birth weight [16] that is consistent with our observations. PUFA-containing triglycerides, particularly those with DHA (FA 22:6), were negatively associated lipids with the sSAT and IAT depots. Fetal lipoprotein lipase (LPL) serves as a key enzyme in triglyceride hydrolysis, facilitating FFA uptake into developing tissues, particularly in adipose tissue along with muscle

and placenta [28]. During fetal development, both SAT and VAT compartments function as primary triglyceride storage depots. Cord blood triglycerides demonstrate an inverse relationship with birth weight, potentially mediated by variations in fetal LPL activity. However, the differential expression of LPL activity across distinct fetal fat depots remains undefined, making the mechanistic relationship between depot-specific LPL activity, cord blood triglyceride levels, and fat depot volumes speculative.

Sexual dimorphism in physiological functions and fat/hormone patterns originates in fetal life [29]. Our findings reveal significant sexual dimorphism in lipid-adipose tissue associations at birth, with girls exhibiting notably stronger interactions between sSAT and dSAT volumes and ether lipids. The observed sex-specific differences in PC-plasmalogens, particularly PC(P-17:0/20:4) and PC(P-16:0/20:4), point to potential variations in peroxisomal function and PPAR signaling between sexes. These ether lipids may influence adipose tissue development through their role as PPARγ ligands, a nuclear receptor essential for adipocyte differentiation and function [30]. Further, plasmalogens contain polyunsaturated fatty acids (PUFA) including essential fatty acids ARA and DHA that are involved in a number of developmental processes particularly that of retina and brain development [31, 32]. PUFAs released from plasmalogen by phospholipase A_2 (PLA_2) play a role as precursors of leukotriens, thromboxanes, and prostaglandins which are potent autocrine and paracrine mediators [33].

Notably, lysophospholipids containing polyunsaturated fatty acids (linolenic acid, DPA, and DHA) showed the strongest lipid × sex interactions, with negative relationships in boys and positive relationships in girls. LPCs are known to be involved in inter-tissue signaling, inflammation [34], and the pathophysiology of obesity [35, 36]. The sex-specific relationship of LPC with body fat depots in boys could be attributed to increased PLA_2 activity in adipose tissues, involving the Lands cycle [37]. These findings suggest that sSAT may actively contribute to sexually dimorphic regulation of metabolic state from fetal and neonatal stages, contrary to previous assumptions of it being metabolically inert.

Among the TG species exhibiting sexual dimorphism, TG(O-52:2) (NL-16:0), showed interactions with sSAT and IAT but not with dSAT. Ether-linked triglycerides have been linked to beige adipocyte development and white adipocyte accumulation, as highlighted by the role of breast milk-derived alkylglycerols in sustaining beige adipocytes through adipose tissue macrophages [38]. Ceramides showed prominent lipid × sex interactions with IAT volume, displaying opposite directional relationships between boys and girls. Given that ceramides modulate adipose tissue function, our finding that the ceramide class of lipids showed the strongest sex-specific interactions with IAT volume suggests a role for ceramides in driving sex-specific differences in IAT fat depot development from in utero life. The significance of these observations is supported by increasing evidence of the physiological and pathological effects of ceramides are dependent on the length of their acyl chains [39]. Beginning in fetal life, abdominal fat depots develop distinct metabolic profiles, with dSAT showing an intermediate phenotype between IAT and sSAT. Depot-specific cord blood lipid signatures suggest developmental programming with sexually dimorphic regulatory pathways during fetal development.

Sex-specific differences in adipose tissue distribution have been previously reported in studies involving children [40], and recent studies have highlighted the importance of depot-specific fat distribution in metabolic health [41, 42]. Building on these findings, our analysis of sex-stratified lipid associations revealed complex relationships between tissue fat and plasma lipids, aligning with evidence that fetal programming of body composition begins in utero. In both sexes, dSAT volume showed inverse relationships with cord plasma PI and PE lipid classes, while sSAT showed positive relationships. Further sex-specific differences emerged in sSAT, where girls displayed stronger associations than boys, particularly with LPCs and LPEs. The dSAT analysis revealed even more pronounced sex differences, with boys showing multiple significant associations across various lipid classes (TGs, PCs, PC(P)s, LPCs, and DeoxyCer), while girls showed no significant associations. Notably, we found no significant associations between cord blood lipids and IAT volume in either boys or girls, despite IAT's known metabolic activity in later life. This absence of associations in neonates suggests that at this life-stage, IAT's primary role might be to provide mechanical support by cushioning abdominal organs. Our findings reveal distinct sex-specific patterns in cord blood lipid associations with neonatal fat distribution, demonstrating depot-specific metabolic programming during fetal development. These early lipid signatures and their marked sexual dimorphism provide new insights into the developmental origins of adipose tissue regulation, with implications for understanding metabolic health trajectories from birth onwards.

While our findings provide novel insights into neonatal lipid metabolism and fat depot development, there are a few limitations of the current study that should be considered. Early infancy fat distribution physiology may differ significantly from adults, necessitating longitudinal studies to determine if these lipid-fat depot associations persist throughout the childhood. Although we adjusted for various confounders, factors

such as nutrition, diet, and psycho-emotional aspects were not examined. Additionally, validation across diverse populations would enhance the generalizability of our findings. While the cord blood lipidome provides important insights into early metabolic processes, its implications for long-term disease risk in children are beyond the scope of this study and remain speculative. Despite these limitations, our results offer valuable perspectives on the molecular basis of sexual dimorphism in early childhood adiposity.

Conclusions

We identified circulating lipid signatures associated with individual abdominal fat compartments at the neonatal stage. By performing detailed association and interaction studies, we identified sexual dimorphism in the association of cord blood lipidome with sSAT, dSAT, and IAT that will enhance the current understanding of the molecular basis of adiposity development in early childhood.

Abbreviations

AC	Acylcarnitine
ARA	Arachidonic acid
BMI	Body mass index
BW	Birth weight
CE	Cholesteryl ester
Cer	Ceramide
deoxyCer	Deoxy-ceramide
DG	Diacylglycerol
DHA	Docosahexaenoic acid
dhCer	Dihydroceramide
dSAT	Abdominal deep subcutaneous adipose tissue
FPG	Fasting plasma glucose
GA	Gestational age
GM3	GM3 ganglioside
GUSTO	Growing Up in Singapore Towards healthy Outcomes
Hex2Cer	Dihexosylceramide
Hex3Cer	Trihexosylceramide
HexCer	Monohexosylceramide
IAT	Abdominal internal adipose tissue
LC–MS/MS	Liquid chromatography-mass spectrometry
LPC	Lysophosphatidylcholine
LPC(O)	Lysoalkylphosphatidylcholine
LPC(P)	Lysoalkenylphosphatidylcholine
LPE	Lysophosphatidylethanolamine
LPE(P)	Lysoalkenylphosphatidylethanolamine
LPI	Lysophosphatidylinositol
NL	Neutral loss
PC	Phosphatidylcholine
PC(O)	Alkylphosphatidylcholine
PC(P)	Alkenylphosphatidylcholine
PE	Phosphatidylethanolamine
PE(O)	Alkylphosphatidylethanolamine
PE(P)	Alkenylphosphatidylethanolamine
PG	Phosphatidylglycerol
PI	Phosphatidylinositol
SAT	Abdominal subcutaneous adipose tissue
SM	Sphingomyelin
sSAT	Abdominal superficial subcutaneous adipose tissue
TG	Triacylglycerol
TG(O)	Alkyl-diacylglycerol
VAT	Visceral adipose tissue

Supplementary Information

The online version contains supplementary material available at https://doi.org/10.1186/s12916-025-04030-0.

Additional file 1: Table S1. Analysis of similarities and differences in maternal demographics and clinical characteristics for samples included and excluded from the study. Table S2. Correlations between the different abdominal fat compartments within the sexes. Boys (A) and Girls (B). Table S3. Correlation of fat depots (sSAT, dSAT and IAT) with the total body weight. Table S4. Distinct and shared lipids associated with different fat depots. Table S5. Lipidomic signatures of Lipid x sex interaction. Table S6A. Cord blood plasma lipids (lipid species) associated with individual fat depots independent of sex. Table S6B. Cord blood plasma lipids (lipid classes) associated with individual fat depots independent of sex. Table S6C. Interaction analysis (Lipid Species): We examined whether sex could modify the effect measure by incorporating lipid x sex interaction terms into the corresponding adjusted model for each fat depot. An interaction $p < 0.05$ was used for data interpretation purposes. Table S6D. Interaction analysis (Lipid Classes): We examined whether sex could modify the effect measure by incorporating lipid x sex interaction terms into the corresponding adjusted model for each fat depot. An interaction $p < 0.05$ was used for data interpretation purposes. Table S6E. Sex stratified association analysis (Lipid species): Cord blood plasma lipids (lipid classes) associated with individual fat depots stratified for sex. Table S6F. Sex stratified association analysis (Lipid class): Cord blood plasma lipids (lipid classes) associated with individual fat depots stratified for sex. Table S6G. Cord blood plasma lipids (lipid species) associated with individual fat depots independent of sex (after adjusting for Childbirth Weight in the model). Table S6H. Cord blood plasma lipids (lipid classes) associated with individual fat depots independent of sex (after adjusting for Childbirth Weight in the model). Table S6I. Sex stratified association analysis (Lipid species) after adjusting for Childbirth Weight in the model: Cord blood plasma lipids (lipid classes) associated with individual fat depots stratified for sex. Table S6J. Sex stratified association analysis (Lipid class) after adjusting for Childbirth Weight in the model: Cord blood plasma lipids (lipid classes) associated with individual fat depots stratified for sex. Fig. S1. VENN diagram: Lipids unique and common to fats depots based on association analysis. Fig. S2. VENN diagram: Lipids unique and common to fats depots based on Interaction analysis. Fig. S3. Sensitivity analysis with infants born at 35 weeks and at term (more than 37 weeks). The scatter plots indicate the correlation between the estimates of the association of plasma lipids with sSAT (Fig.S3A), dSAT (Fig.S3B), and IAT (Fig.S3C) body fat depots. Fig. S4. Sex-stratified analysis is presented with Fig. 4A-B displaying forest plots and Fig. 4C-D showing volcano plots representing the associations between sSAT volumes (in mL) and plasma lipidome profiles for lipid species and lipid classes, respectively. The forest plots and volcano plots represent: 1) boy-specific data and 2) girl-specific data. Each square in the forest plots corresponds to an individual lipid species. In both forest plots and volcano plots, red color represents FDR < 0.05, green color represents $p < 0.05$, and grey color indicates nonsignificant associations. Fig. S5. Sex-stratified analysis is presented with Fig. 5A-B displaying forest plots and Fig. 5C-D showing volcano plots representing the associations between dSAT volumes (in mL) and plasma lipidome profiles for lipid species and lipid classes, respectively. The forest plots represent: 1) boy-specific data and 2) girl-specific data. Each square in the forest plots corresponds to an individual lipid species. In both forest plots and volcano plots, red color represents FDR < 0.05, green color represents $p < 0.05$, and grey color indicates nonsignificant associations. Fig. S6. Sex-stratified analysis is presented with Fig. 6A-B displaying forest plots and Fig. 6C-D showing volcano plots representing the associations between IAT volumes (in mL) and plasma lipidome profiles for lipid species and lipid classes, respectively. The forest plots represent: 1) boy-specific data and 2) girl-specific data. Each square in the forest plots corresponds to an individual lipid species. In both forest plots and volcano plots, red color represents FDR < 0.05, green color represents $p < 0.05$, and grey color indicates nonsignificant associations. Fig. S7. Analysis of TAAT and lipid associations. Figure 7A shows a forest plot of linear regression analysis independent of sex between TAAT and log-transformed lipid species concentrations, while Fig. 7B-C present sex-stratified forest plots for these

associations (boy-specific and girl-specific data, respectively). Figure 7D shows a volcano plot of associations with lipid classes independent of sex, while Fig. 7E-F present sex-stratified volcano plots for lipid classes (boy-specific and girl-specific data, respectively). In forest plots, each square corresponds to an individual lipid species, with error bars representing the 95% confidence interval. In both forest plots and volcano plots, red color represents FDR < 0.05, green color represents $p < 0.05$, and grey color indicates nonsignificant associations.

Additional file 2.

Acknowledgements
This study group includes: Airu Chia, Andrea Cremaschi, Anna Magdalena Fogel, Anne Eng Neo Goh, Anne Rifkin-Graboi, Anqi Qiu, Arijit Biswas, Bee Wah Lee, Birit Froukje Philipp Broekman, Candida Vaz, Chai Kiat Chng, Chan Shi Yu, Choon Looi Bong, Daniel Yam Thiam Goh, Dawn Xin Ping Koh, Dennis Wang, Desiree Y. Phua, E Shyong Tai, Elaine Kwang Hsia Tham, Elaine Phaik Ling Quah, Elizabeth Huiwen Tham, Evelyn Chung Ning Law, Evelyn Keet Wai Lau, Evelyn Xiu Ling Loo, Falk Müller-Riemenschneider, Franzolini Beatrice, George Seow Heong Yeo, Gerard Chung Siew Keong, Hannah Ee Juen Yong, Helen Yu Chen, Huang Jian, Huang Pei, Hugo P S van Bever, Hui Min Tan, Iliana Magiati, Inez Bik Yun Wong, Ives Lim Yubin, Ivy Yee-Man Lau, Jacqueline Chin Siew Roong, Jadegoud Yaligar, Jerry Kok Yen Chan, Jia Xu, Jonathan Tze Liang Choo, Jonathan Y. Bernard, Jonathan Yinhao Huang, Joshua J. Gooley, Jun Shi Lai, Keith M. Godfrey, Keri McCrickerd, Kok Hian Tan, Krishnamoorthy Naiduvaje, Kuan Jin Lee, Li Chen, Lieng Hsi Ling, Lin Lin Su, Ling-Wei Chen, Lourdes Mary Daniel, Lynette Pei-Chi Shek, Maria De Iorio, Marielle V. Fortier, Mary Foong-Fong Chong, Mary Wlodek, Mei Chien Chua, Melvin Khee-Shing Leow, Michael J. Meaney, Michelle Zhi Ling Kee, Min Gong, Ngee Lek, Noor Hidayatul Aini Bte Suaini, Ong Yi Ying, Oon Hoe Teoh, Queenie Ling Jun Li, Seang Mei Saw, See Ling Loy, Seng Bin Ang, Shang Chee Chong, Shirong Cai, Shu-E Soh, Stephen Chin-Ying Hsu, Swee Chye Quek, Tan Ai Peng, Varsha Gupta, Victor Samuel Rajadurai, Wee Meng Han, Wei Wei Pang, Yin Bun Cheung, Yiong Huak Chan, Yung Seng Lee, Zhang Han.

Authors' contributions
KN, MRW, SAM, and LC conceived and supervised the study. MTT and KMLT contributed to the data and sample collection. KN, AR, LC, MRW, SAS, and NM performed the experimental work, experimental design, pre-processing and quality control, and carried out the statistical analysis and association studies. KN, LC, SAM, SAS, NM, CSY, and MRW interpreted the results and wrote the manuscript. NK, KMLT, PM, AKB, TKH, DCS, YSC, PDG, PJM, MKSL, FY, YSL, JGE, and SSV reviewed and provided critical feedback on the manuscript. All authors read and approved the final manuscript.

Funding
This work was supported by the Translational Clinical Research (TCR) Flagship Program on Developmental Pathways to Metabolic Disease funded by the National Research Foundation (NRF) and administered by the National Medical Research Council (NMRC), Singapore—NMRC/TCR/004-NUS/2008 provided the funding support for subject recruitment and sample and data collection in GUSTO cohort study. The Singapore Lipidomics Incubator (SLING) is supported by grants from the National University of Singapore via the Life Sciences Institute, the National Research Foundation (NRF, NRFI2015-05 and NRFSBP-P4), and the NRF and A*STAR IAF-ICP I1901E0040.

Data availability
The data supporting the findings and figures in this study are available in the supplementary materials. Due to ethical restrictions, the data are not publicly accessible but can be requested from the authors. Access is contingent upon obtaining appropriate approvals, including from the GUSTO cohort's Executive Committee.

Declarations

Ethics approval and consent to participate
Written informed consent was obtained at recruitment, and ethics approval for the study was granted by the Institute Review Boards of both KK Women's and Children's Hospital (KKH) and National University Hospital (NUH), which are the Centralised Institutional Review Board of SingHealth (CIRB) under CIRB Ref: 2018/2767 and the Domain Specific Review Board of Singapore National Healthcare Group (DSRB) under DSRB Ref: D/2009/021. This study was registered under ClinicalTrials.gov on 1 July 2010 under the identifier NCT01174875. The study was conducted in accordance with the Declaration of Helsinki, and the lipidomics study was approved by the Institutional Review Board of National University of Singapore # H-17-055E.

Consent for publication
NA.

Competing interests
NK and YSC are part of an academic consortium that has received research funding from Abbott Nutrition, Nestec, EVOLVE Biosystems, DSM, and Danone. All other authors declare that they have no competing interests.

Author details
[1]Institute for Human Development and Potential (IHDP), Agency for Science, Technology and Research (A*STAR), Brenner Centre for Molecular Medicine, 30 Medical Drive, Singapore 117609, Singapore. [2]Life Sciences Institute, Singapore Lipidomics Incubator, National University of Singapore, Singapore, Singapore. [3]Department of Biochemistry, Yong Loo Lin School of Medicine, National University of Singapore, Singapore, Singapore. [4]Agency for Science, Technology and Research (A*STAR), Genome Institute of Singapore (GIS), 60 Biopolis Street, Genome, Singapore 138672, Republic of Singapore. [5]Maternal Fetal Medicine, KK Women's and Children's Hospital (KKH), Singapore, Singapore. [6]Singapore Institute of Food and Biotechnology Innovation (SIFBI), Agency for Science, Technology and Research (A*STAR), 14 Medical Drive, MD6, #07-02 Singapore, Singapore. [7]Department of Obstetrics and Gynaecology and Human Potential Translational Research programme, Yong Loo Lin School of Medicine, National University of Singapore, Singapore, Singapore. [8]Centre for Human Evolution, Adaptation and Disease, Liggins Institute, University of Auckland, Auckland, New Zealand. [9]Baker Heart and Diabetes Institute AU, Melbourne, VIC 3004, Australia. [10]Department of Cardiovascular Research, Translation and Implementation, La Trobe University, Bundoora, VIC 3086, Australia. [11]Lee Kong Chian School of Medicine, Nanyang Technological University, Singapore, Singapore. [12]Department of Endocrinology, Tan Tock Seng Hospital, Singapore, Singapore. [13]Cardiovascular and Metabolic Disorders Program, Duke-NUS Medical School, Singapore, Singapore. [14]Division of Paediatric Medicine, KK Women's and Children's Hospital, Singapore, Singapore. [15]Department of Paediatrics, Yong Loo Lin School of Medicine, National University of Singapore, Singapore, Singapore. [16]Folkhalsan Research Center, Helsinki, Finland. [17]Department of General Practice and Primary Health Care, University of Helsinki, Helsinki, Finland. [18]Clinical Data Engagement, Bioinformatics Institute, Agency for Science Technology and Research (A*STAR), Singapore, Singapore. [19]College of Health and Life Sciences, Hamad Bin Khalifa University, Doha, Qatar.

Received: 27 June 2024 Accepted: 21 March 2025
Published online: 14 April 2025

References

1. Tint MT, Fortier MV, Godfrey KM, Shuter B, Kapur J, Rajadurai VS, et al. Abdominal adipose tissue compartments vary with ethnicity in Asian neonates: Growing Up in Singapore Toward Healthy Outcomes birth cohort study. Am J Clin Nutr. 2016;103(5):1311–7.
2. Davis SM, Kaar JL, Ringham BM, Hockett CW, Glueck DH, Dabelea D. Sex differences in infant body composition emerge in the first 5 months of life. J Pediatr Endocrinol Metab. 2019;32(11):1235–9.
3. Boulet N, Briot A, Galitzky J, Bouloumie A. The Sexual Dimorphism of Human Adipose Depots. Biomedicines. 2022;10(10):2615.
4. Burugupalli S, Smith AAT, Oshlensky G, Huynh K, Giles C, Wang T, et al. Ontogeny of circulating lipid metabolism in pregnancy and early childhood - a longitudinal population study. Elife. 2022;11:e72779.
5. Hellmuth C, Uhl O, Standl M, Demmelmair H, Heinrich J, Koletzko B, et al. Cord Blood Metabolome Is Highly Associated with Birth Weight, but Less Predictive for Later Weight Development. Obes Facts. 2017;10(2):85–100.
6. West AL, Michaelson LV, Miles EA, Haslam RP, Lillycrop KA, Georgescu R, et al. Lipidomic Analysis of Plasma from Healthy Men and Women Shows

Phospholipid Class and Molecular Species Differences between Sexes. Lipids. 2021;56(2):229–42.
7. Beyene HB, Olshansky G, AA TS, Giles C, Huynh K, Cinel M, et al. High-coverage plasma lipidomics reveals novel sex-specific lipidomic fingerprints of age and BMI: Evidence from two large population cohort studies. PLoS Biol. 2020;18(9):e3000870.
8. Slade E, Irvin MR, Xie K, Arnett DK, Claas SA, Kind T, et al. Age and sex are associated with the plasma lipidome: findings from the GOLDN study. Lipids Health Dis. 2021;20(1):30.
9. Costanzo M, Caterino M, Sotgiu G, Ruoppolo M, Franconi F, Campesi I. Sex differences in the human metabolome. Biol Sex Differ. 2022;13(1):30.
10. Tabassum R, Widen E, Ripatti S. Effect of biological sex on human circulating lipidome: An overview of the literature. Atherosclerosis. 2023;384:117274.
11. Karsai G, Lone M, Kutalik Z, Brenna JT, Li H, Pan D, et al. FADS3 is a Delta14Z sphingoid base desaturase that contributes to gender differences in the human plasma sphingolipidome. J Biol Chem. 2020;295(7):1889–97.
12. Desoye G, Herrera E. Adipose tissue development and lipid metabolism in the human fetus: The 2020 perspective focusing on maternal diabetes and obesity. Prog Lipid Res. 2021;81:101082.
13. Ye QQ, Kong SM, Yin X, Gao C, Lu MS, Ramakrishnan R, et al. Associations of Cord Blood Lipids with Childhood Adiposity at the Age of Three Years: A Prospective Birth Cohort Study. Metabolites. 2022;12(6):522.
14. Soh SE, Tint MT, Gluckman PD, Godfrey KM, Rifkin-Graboi A, Chan YH, et al. Cohort profile: Growing Up in Singapore Towards healthy Outcomes (GUSTO) birth cohort study. Int J Epidemiol. 2014;43(5):1401–9.
15. Chen LW, Soh SE, Tint MT, Loy SL, Yap F, Tan KH, et al. Combined analysis of gestational diabetes and maternal weight status from pre-pregnancy through post-delivery in future development of type 2 diabetes. Sci Rep. 2021;11(1):5021.
16. Mir SA, Chen L, Burugupalli S, Burla B, Ji S, Smith AAT, et al. Population-based plasma lipidomics reveals developmental changes in metabolism and signatures of obesity risk: a mother-offspring cohort study. BMC Med. 2022;20(1):242.
17. Tint MT, Sadananthan SA, Soh SE, Aris IM, Michael N, Tan KH, et al. Maternal glycemia during pregnancy and offspring abdominal adiposity measured by MRI in the neonatal period and preschool years: The Growing Up in Singapore Towards healthy Outcomes (GUSTO) prospective mother-offspring birth cohort study. Am J Clin Nutr. 2020;112(1):39–47.
18. Benjamini Y HY. Controlling the False Discovery Rate: A Practical and Powerful Approach to Multiple Testing. J Royal Stat Soc Series B (Methodological) 1995;57(1);289–300.
19. Wickham H. ggplot2: Elegant Graphics for Data Analysis. Springer-Verlag New York. . 2016;ISBN 978–3–319–24277–4.
20. Schisterman EF, Cole SR, Platt RW. Overadjustment bias and unnecessary adjustment in epidemiologic studies. Epidemiology. 2009;20(4):488–95.
21. Wong G, Narasimhan K, Cheong WF, Ng S, Aris IM, Loy SL, et al. Umbilical Cord Plasma Lysophospholipids and Triacylglycerols Associated with Birthweight Percentiles. Nutrients. 2024;16(2):274.
22. Chassen SS, Zemski-Berry K, Raymond-Whish S, Driver C, Hobbins JC, Powell TL. Altered Cord Blood Lipid Concentrations Correlate with Birth Weight and Doppler Velocimetry of Fetal Vessels in Human Fetal Growth Restriction Pregnancies. Cells. 2022;11(19).
23. Zheng J, Lam SM, Jiang B, Mao L, Liu J, Zhang Q, et al. Cord blood ceramides facilitate early risk identification into childhood metabolic health. Natl Sci Rev. 2024;11(10):nwae352.
24. Schaefer-Graf UM, Graf K, Kulbacka I, Kjos SL, Dudenhausen J, Vetter K, et al. Maternal lipids as strong determinants of fetal environment and growth in pregnancies with gestational diabetes mellitus. Diabetes Care. 2008;31(9):1858–63.
25. Herrera E, Desoye G. Maternal and fetal lipid metabolism under normal and gestational diabetic conditions. Horm Mol Biol Clin Investig. 2016;26(2):109–27.
26. Lu YP, Reichetzeder C, Prehn C, Yin LH, Yun C, Zeng S, et al. Cord Blood Lysophosphatidylcholine 16: 1 is Positively Associated with Birth Weight. Cell Physiol Biochem. 2018;45(2):614–24.
27. Yea K, Kim J, Yoon JH, Kwon T, Kim JH, Lee BD, et al. Lysophosphatidylcholine activates adipocyte glucose uptake and lowers blood glucose levels in murine models of diabetes. J Biol Chem. 2009;284(49):33833–40.
28. Weinstock PH, Levak-Frank S, Hudgins LC, Radner H, Friedman JM, Zechner R, et al. Lipoprotein lipase controls fatty acid entry into adipose tissue, but fat mass is preserved by endogenous synthesis in mice deficient in adipose tissue lipoprotein lipase. Proc Natl Acad Sci U S A. 1997;94(19):10261–6.
29. Wells JC. Sexual dimorphism of body composition. Best Pract Res Clin Endocrinol Metab. 2007;21(3):415–30.
30. Dean JM, Lodhi IJ. Structural and functional roles of ether lipids. Protein Cell. 2018;9(2):196–206.
31. Saab S, Buteau B, Leclere L, Bron AM, Creuzot-Garcher CP, Bretillon L, et al. Involvement of plasmalogens in post-natal retinal vascular development. PLoS ONE. 2014;9(6):e101076.
32. Sinclair AJ. Docosahexaenoic acid and the brain- what is its role? Asia Pac J Clin Nutr. 2019;28(4):675–88.
33. Maloberti P, Cornejo Maciel F, Castillo AF, Castilla R, Duarte A, Toledo MF, et al. Enzymes involved in arachidonic acid release in adrenal and Leydig cells. Mol Cell Endocrinol. 2007;265–266:113–20.
34. Sevastou I, Kaffe E, Mouratis MA, Aidinis V. Lysoglycerophospholipids in chronic inflammatory disorders: the PLA(2)/LPC and ATX/LPA axes. Biochim Biophys Acta. 2013;1831(1):42–60.
35. Heimerl S, Fischer M, Baessler A, Liebisch G, Sigruener A, Wallner S, et al. Alterations of plasma lysophosphatidylcholine species in obesity and weight loss. PLoS ONE. 2014;9(10):e111348.
36. Bellot P, Moia MN, Reis BZ, Pedrosa LFC, Tasic L, Barbosa F Jr, et al. Are Phosphatidylcholine and Lysophosphatidylcholine Body Levels Potentially Reliable Biomarkers in Obesity? A Review of Human Studies. Mol Nutr Food Res. 2023;67(7):e2200568.
37. Law SH, Chan ML, Marathe GK, Parveen F, Chen CH, Ke LY. An Updated Review of Lysophosphatidylcholine Metabolism in Human Diseases. Int J Mol Sci. 2019;20(5):1149.
38. Yu H, Dilbaz S, Cossmann J, Hoang AC, Diedrich V, Herwig A, et al. Breast milk alkylglycerols sustain beige adipocytes through adipose tissue macrophages. J Clin Invest. 2019;129(6):2485–99.
39. Grosch S, Schiffmann S, Geisslinger G. Chain length-specific properties of ceramides. Prog Lipid Res. 2012;51(1):50–62.
40. Gale C, Logan KM, Jeffries S, Parkinson JR, Santhakumaran S, Uthaya S, et al. Sexual dimorphism in relation to adipose tissue and intrahepatocellular lipid deposition in early infancy. Int J Obes (Lond). 2015;39(4):629–32.
41. Yan Y, Liu J, Zhao X, Cheng H, Huang G, Mi J, et al. Abdominal visceral and subcutaneous adipose tissues in association with cardiometabolic risk in children and adolescents: the China Child and Adolescent Cardiovascular Health (CCACH) study. BMJ Open Diabetes Res Care. 2019;7(1):e000824.
42. Staiano AE, Gupta AK, Katzmarzyk PT. Cardiometabolic risk factors and fat distribution in children and adolescents. J Pediatr. 2014;164(3):560–5.

Publisher's Note